BER the international journal of bridge engineering management and research

A Novel Quantitative Approach for Multi-Hazard Risk Assessment of Linear Infrastructure: A Geological-Geotechnical Index

Nadia Salvatore[1,*]; Alessandro Pagliaroli[2]; and Giuseppe Brando[3]

Submitted: 08 January 2025 **Accepted:** 18 March 2025 **Publication date:** 10 April 2025

DOI: 10.70465/ber.v2i2.24

Abstract: This study introduces a novel quantitative approach for multi-hazard risk assessment of linear infrastructure by introducing the GEological-geoTechnical Index (GETI). GETI aims to address the limitations of existing methodologies by incorporating the cascading effects of multiple hazards and providing a comprehensive quantitative assessment tool for stakeholders. This study highlights the challenges in maintaining linear infrastructure, such as bridges and viaducts, and the necessity for standardized procedures to assess their exposure to natural hazards. Current approaches often fail to account for the interconnected nature of multiple hazards, potentially leading to underestimation of risks. The GETI is conceptualized as a two-level analysis process. Level 1 involves assessing hazard susceptibility through a literature review and preliminary surveys, whereas Level 2 encompasses advanced analyses using geological and geotechnical data. The index primarily addresses seismic risk and its secondary effects, including ground motion amplification, soil liquefaction, and landslides/rockfalls. This methodology employs conditional probability to express the concept of the "cascade effect" in mathematical terms. The GETI is formulated as the probability of damage given the occurrence of an earthquake, considering various magnitudes of damage, from low to severe. This approach allows for a more nuanced understanding of risk compared to qualitative or semiquantitative indices. This study acknowledges the potential limitations of the GETI, including its dependence on data availability and accuracy, as well as its current focus on seismic hazards. Future research directions are proposed, such as expanding the index to include a broader spectrum of natural hazards and extending its applicability to other types of linear infrastructure. The GETI represents a significant advancement in multi-hazard risk assessment for linear infrastructure. By providing a quantitative measure that accounts for the interrelated nature of natural hazards, it offers stakeholders a valuable tool for prioritizing risk-reduction measures and ensuring the safety and resilience of critical infrastructure. The practical application of GETI in a case study in Italy is finally presented to verify its real-world functionality and effectiveness in infrastructure management.

Author keywords: Multi-hazard risk assessment; Linear infrastructure; Quantitative index; Seismic hazards; Conditional probability

*Corresponding Author: Nadia Salvatore.
Email: nadia.salvatore@phd.unict.it

[1]Department of Civil Engineering and Architecture, University of Catania, via Santa Sofia, 64, 95123 Catania, Italy; Department of Engineering and Geology, University "G. d'Annunzio" of Chieti-Pescara, viale Pindaro, 42, 65129, Pescara, Italy

[2]Department of Engineering and Geology, University "G. d'Annunzio" of Chieti-Pescara, viale Pindaro, 42, 65129 Pescara, Italy; Istituto di Geologia Ambientale e Geoingegneria (IGAG)–Consiglio Nazionale delle Ricerche, Roma, Italy

[3]Department of Engineering and Geology, University "G. d'Annunzio" of Chieti-Pescara, viale Pindaro, 42, 65129 Pescara, Italy; UdA-TechLab, Research Center, University "G. d'Annunzio" of Chieti-Pescara, 66100, Chieti, Italy

Discussion period open till six months from the publication date. Please submit separate discussion for each individual paper. This paper is a part of the Vol. 2 of the International Journal of Bridge Engineering, Management and Research (© BER), ISSN 3065-0569.

Introduction

The maintenance of linear infrastructure, such as viaducts or bridges, whether masonry or reinforced concrete structures, presents a significant challenge for stakeholders.

To ensure the safety of citizens, governments worldwide have developed standardized procedures for assessing the state of maintenance and exposure to natural hazards, utilizing qualitative and semiquantitative indices to express the overall risk associated with a given infrastructure.[1–4] Despite the existing multi-risk-based methodologies for linear infrastructure, current approaches often fail to account for the cascading effects derived from multiple hazards. To address the limitations of existing methodologies, this study proposes the development of the GEological-geoTechnical

Index (GETI), a novel quantitative approach to risk assessment referred to linear infrastructure in a multi-hazard view.

The GETI index is designed and studied to overcome the limitations of other indices currently found in the literature and used both in Italy and abroad, both in terms of risk analysis from a multi-hazard perspective and in terms of providing facility managers with a net, clear numerical figure that can represent the natural hazard risk associated with a linear structure as accurately as possible.

The GETI index aims to (1) provide a quantitative assessment of the risk to linear infrastructure from multiple interrelated hazards, (2) incorporate the cascade effect of such hazards, and (3) offer a tool for stakeholders to prioritize risk reduction measures based on a comprehensive quantitative assessment. Despite existing methodologies for risk assessment applied to linear infrastructure, there remains a lack of comprehensive tools that consider the potential impact of natural hazards intended to interact with each other and are expressed as a mathematical function. This study proposes the GETI as a solution to this gap. The current version of the GETI primarily addresses seismic risk and its secondary effects. The theoretical formulation of the GETI is currently being applied in practice in at least two selected case studies in Italy and the United States to verify the applicability and real-world functionality of the index.

This article proposes a comprehensive overview of the multi-hazard concept and related indices, as well as the multi-hazard risk assessment of road bridges and viaducts, followed by the theoretical formulation of the GETI index. As a conclusion, the advantages and shortcomings of the index are proposed and discussed.

State-of-the-Art

Since the GETI is based on the concept of "multi-hazard," it is important to give this term an unambiguous definition, considering the wide available literature.

A first definition was the "all-hazards-at-a-place" concept, which involves the identification of all potential hazards,[5] encompassing all natural or anthropogenic conditions that possess the potential to inflict damage on exposed assets in a specified area.

The concept of "multi-hazard" initially emerged in the United Nations Agenda 21 for sustainable development[6] and was subsequently defined comprehensively by Kappes[7] as "the totality of relevant hazards in a defined area," considering as "relevant" those hazardous processes that cause a certain level of damage depending on the specific geological and social settings, the target of the study, and the importance and characteristics of the infrastructure. Conversely, if a hazard causes damage below a certain threshold, it is considered insignificant. Greiving et al.[8] contributed to this perspective by defining "relevant" hazardous processes as those with a significant probability of occurring in the specified area. In this view, events of extremely low probability of occurrence, such as meteorite impacts, are excluded.

When considering the problem through a thematic approach, hazards can be conceptualized not as isolated processes but as multiple interconnected processes,[9] considering that, in certain instances, one hazard may trigger or interact with other hazardous phenomena (e.g., rockfalls or liquefaction induced by seismic activity). Gill and Malamud[10] conducted a comprehensive global literature review to elucidate the potential interactive relationships among twenty-one natural hazards, categorized into six hazard groups (geophysical, hydrological, shallow Earth, atmospheric, biophysical, and space hazards). In this way, they developed a Hazard Interaction Matrix by considering four distinct interaction categories: interactions in which a hazard is triggered (cascade effect), interactions that increase the probability of a hazard, interactions that decrease the probability of a hazard, and events involving the spatial and temporal coincidence of natural hazards (e.g., an earthquake during a strong rainstorm; events are not causally linked, but their simultaneous occurrence represents a multi-hazard scenario). This study provides valuable insights into the occurrence of natural hazards.

To build our definition of multi-hazard, we next explore how this concept informs the development of both qualitative and quantitative risk assessment indices. The first category encompasses the Italian *Guidelines for risk classification and management, safety assessment, and structural health monitoring of existing bridges*, established by the Ministero delle Infrastrutture e delle Mobilità Sostenibili.[3,11] This framework employs a multilevel approach comprising four stages: Level 0, which involves a document-based examination of the infrastructure and the surrounding area; Level 1, which entails a field survey concerning geological-geomorphological observations of the site and a reconnaissance of structural defects and general maintenance conditions; and Level 2, which consists of an analysis of the data collected at Levels 0 and 1, resulting in a "warning class," graded on five possible qualitative judgments (High, Medium-High, Medium, Medium-Low, and Low) (see Fig. 1) with respect to four types of risks—Structural and Foundation Risk, Seismic Risk, Landslide Risk, and Hydraulic Risk—to prioritize those infrastructures that are deemed to be worthy of more detailed analyses for implementing effective mitigation measures. Each type of risk is evaluated independently, incorporating the results of the defectivity analysis. The primary focus is on landslides and hydraulic hazards, whereas seismic hazard assessment is limited to qualitative evaluation based on peak ground acceleration (PGA) and the moment magnitude (M_W) expected in the area.

Infrastructure categorized in classes from "medium" to "high" is subjected to Levels 3 and 4, which entail a more detailed evaluation in accordance with the Italian building code,[12] and in select cases, to a Level 5, applied exclusively to a specific type of infrastructure.

Consequently, the "warning class" derived from Levels 1 and 2 is evaluated and revised as necessary with the support of quantitative analyses, incorporating data from new surveys and monitoring activities.

Another significant example of a qualitative index is the National Risk Index, developed by the U.S. Department of

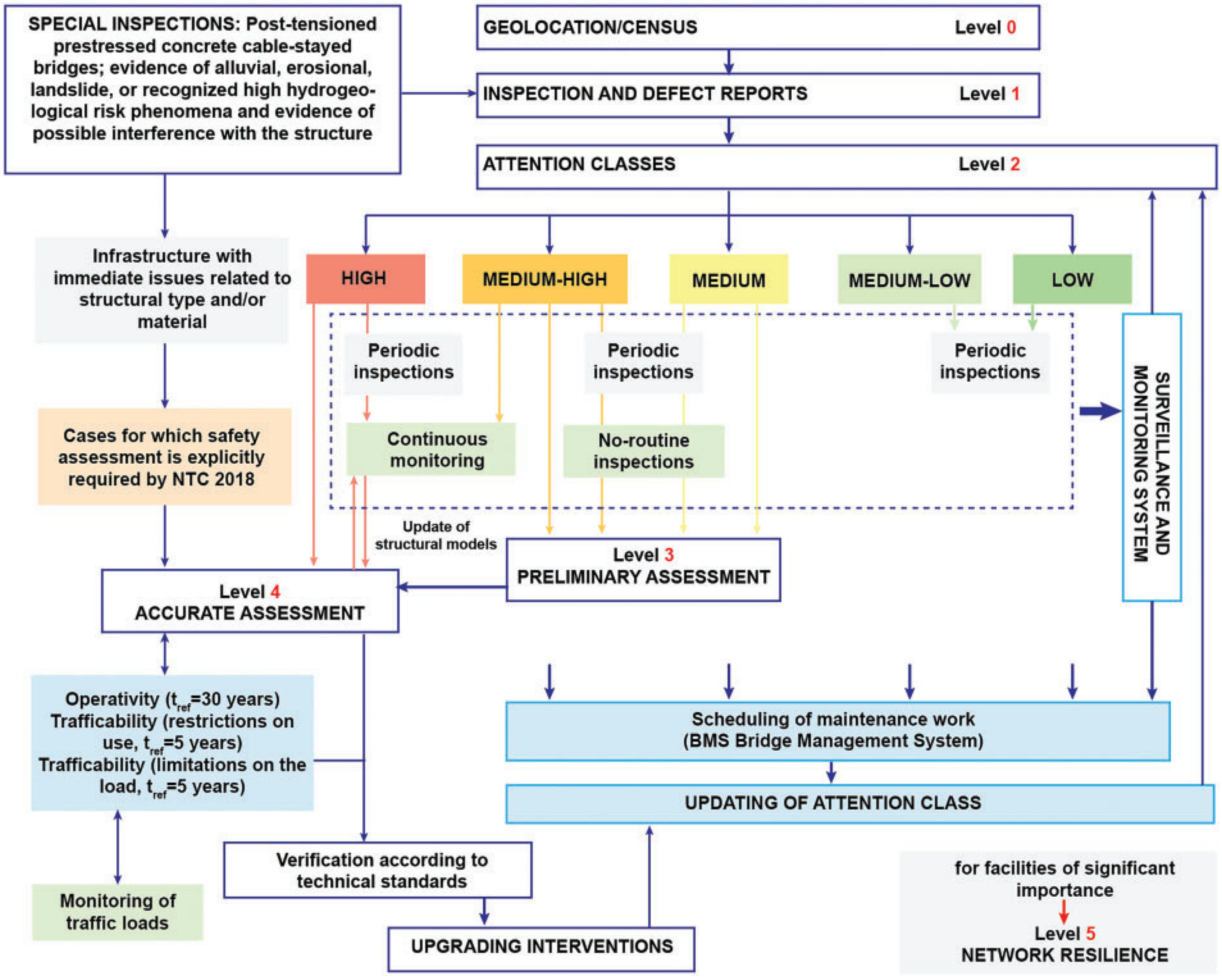

Figure 1. Logic flowchart of the Italian *Guidelines for risk classification and management, safety assessment, and monitoring of existing bridges* (modified from MIMS[3])

Homeland Security,[4] which is defined as the product of the Expected Annual Loss (EAL) and the Social Vulnerability Index (SoVI), divided by the community resilience score. This index, even though qualitative, attempts to quantify the impact of all natural hazards that can affect regions in the United States related to social vulnerability, also intended as the resilience of infrastructure. The vulnerability of linear infrastructure, such as road bridges and viaducts, is considered in this broader concept and has not been analyzed in detail.

According to the methodology proposed by FEMA, the composite EAL value is determined by combining the EAL values for each hazard type.

A composite Risk Index can be calculated using the same methodology as the composite EAL, normalizing the EAL, SoVI, and community resilience scores to a range from 0 (lowest possible value) to 100 (highest possible value) to facilitate their combination.[13]

Subsequently, a composite, multi-hazard risk index score is computed, representing the risk of a community for all hazard types relative to all other communities at the same level, expressed in a five-category qualitative rating ranging from "very low" to "very high."

In summary, in qualitative indices, the intensity and frequency thresholds are typically established to categorize hazards into a predefined number of classes. This approach facilitates hazard comparability, albeit within a qualitative framework of, for instance, "high hazard." Consequently, this methodology allows for the generation of hazard maps through the superimposition of classification results for individual hazards, considering the highest hazard class when multiple scenarios of the same process or different processes overlap.[14]

As an example, the Italian *Guidelines for risk classification and management, safety assessment, and monitoring of existing bridges*[3] show the limitations of this approach. The impact of natural hazards on infrastructure could be underestimated because hydraulic, seismic, and landslide/rockfall hazards are analyzed as if they were phenomena of their own, without consideration of the dynamics of the "cascade effect" and, consequently, of other hazards that may trigger or influence them. This appears to be evident in recent decades when natural hazards derived from earthquakes and climate change have had a dramatic impact on the Italian region. For example, consider the case of a road bridge near the town of Rotella (Ascoli Piceno, Italy), which was seriously damaged by an earthquake-induced landslide during the M_W 6.5 Norcia earthquake of 2016 and is still not accessible,[15] and a road bridge near Ozzanello (Parma, Italy) that collapsed during intense rainfall in October 2023 due to the load caused by the flood from the Sporzana River.[16]

Moreover, the results of the analyses of Levels 0, 1, and 2 are mostly affected by the superimposition of the warning classes related to natural hazards with the warning class related to the structure, based on defectivity, which does not allow for a clear view of the potential impact of natural hazards on the structure under consideration. In other words, in the first levels of the analysis, the behavior of the structure under the action imposed by natural phenomena is not evaluated.

To make a stepforward, quantitative indices can be considered. In this approach, the output data of the natural risk assessment is not a superimposition of the warning classes derived for each phenomenon, but a quantification in mathematical terms of the impact of natural hazards on a certain region, considering the vulnerability of structures to each hazard. An example is the hazard score (HS) proposed by Odeh[17] for risk assessment from a multi-hazard perspective. The index considers each individual hazard that could affect a given area and quantifies it through the average number of events per year (frequency score), percentage of subregions or the average impact in square miles of the event considered (scope score), and level of intensity (intensity score).

The HS is calculated using the following equation:

$$HS = F \cdot S \cdot I \tag{1}$$

where F is the frequency score, S is the scope score, and I is the intensity score.

To compute the multi-HS, the HS values calculated for each identified hazard in the area were aggregated. The resulting HS is a continuous measure owing to the multiplicity of the classified input scores. One limitation of this approach is that it does not provide information on the spatial distribution of hazards or risks to communities at this level. Furthermore, this method considers only multiple hazards as the sum of individual hazards.

A few years later, Dilley et al.[18] proposed a simple multi-hazard index composed of single-hazard analyses. Hazards were investigated through the integration of historical event data and modeling techniques. The final index value is derived from the sum of the individual hazard indices, which falls within the range of 8–10. The limitation of this index value is that it is semiquantitative because the risk is expressed in warning classes, even though the analysis is conducted using a statistical approach and natural hazards are deduced from historical data. However, the spatial distribution of hazards is considered, even if the contribution of each phenomenon is not connected to the others.

In summary, quantitative indices can provide a continuous standardization of diverse and not directly comparable parameters, enabling the quantification of differences between hazard levels rather than merely ranking them, as seen with qualitative indices. Thus, it is possible to overcome one of the limitations of qualitative indices, despite this approach still being limited to one-by-one hazards.

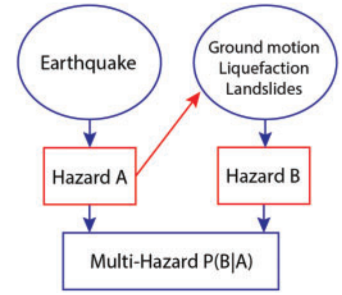

Figure 2. Schematization of the multi-hazard concept (modified from Gill and Malamud[10])

Theoretical Formulation of the Geti Index

Given these findings, we propose a novel quantitative index for linear infrastructure risk assessment within a multi-hazard framework. This index uniquely accounts for the "cascade effect" of natural hazards and offers a viable method for comprehensively assessing infrastructure exposure.

The GETI is based on the multi-hazard concept related to the conditional probability of the occurrence of secondary phenomena directly or indirectly related to the primary hazard taken into account (Fig. 2).

Because of the complexity of the natural system, as highlighted by Gill and Malamud,[10] a simplified approach was adopted to facilitate the development of the GETI index. Consequently, accounting for all primary natural hazards that occurred in Italy and are reported in historical and geological records,[19,20] only seismic risk is considered in this study, and the susceptibility of a specific area to ground seismic motion amplification (S), soil liquefaction (LQ), and landslides/rockfalls (L) is evaluated as a secondary effect of an earthquake.[21–23]

Therefore, the GETI is structured as the conditional probability of damage to linear infrastructure induced by an earthquake (primary hazard) and its secondary effects (secondary hazards). This simplification enables a more comprehensive understanding of the functionality of the index, making its application to ongoing case studies simpler. Future applications will expand the index to other natural hazards.

The GETI is designed as a quantitative multi-hazard index conceptualized in two levels of analysis. This can be defined as the conditional probability of damage related to linear infrastructure, primarily bridges and viaducts. The logic flow that leads to the GETI is shown in Fig. 3.

Level 1—assessing hazards susceptibility—structural and geological knowledge

From a multi-hazard perspective, the initial level of the logical process for calculating the GETI index aims to examine the susceptibility of a specific area to natural hazards that may impact the linear structure located therein.

The first step, Level 1, begins with a thorough review of existing literature, including scientific studies, reports,

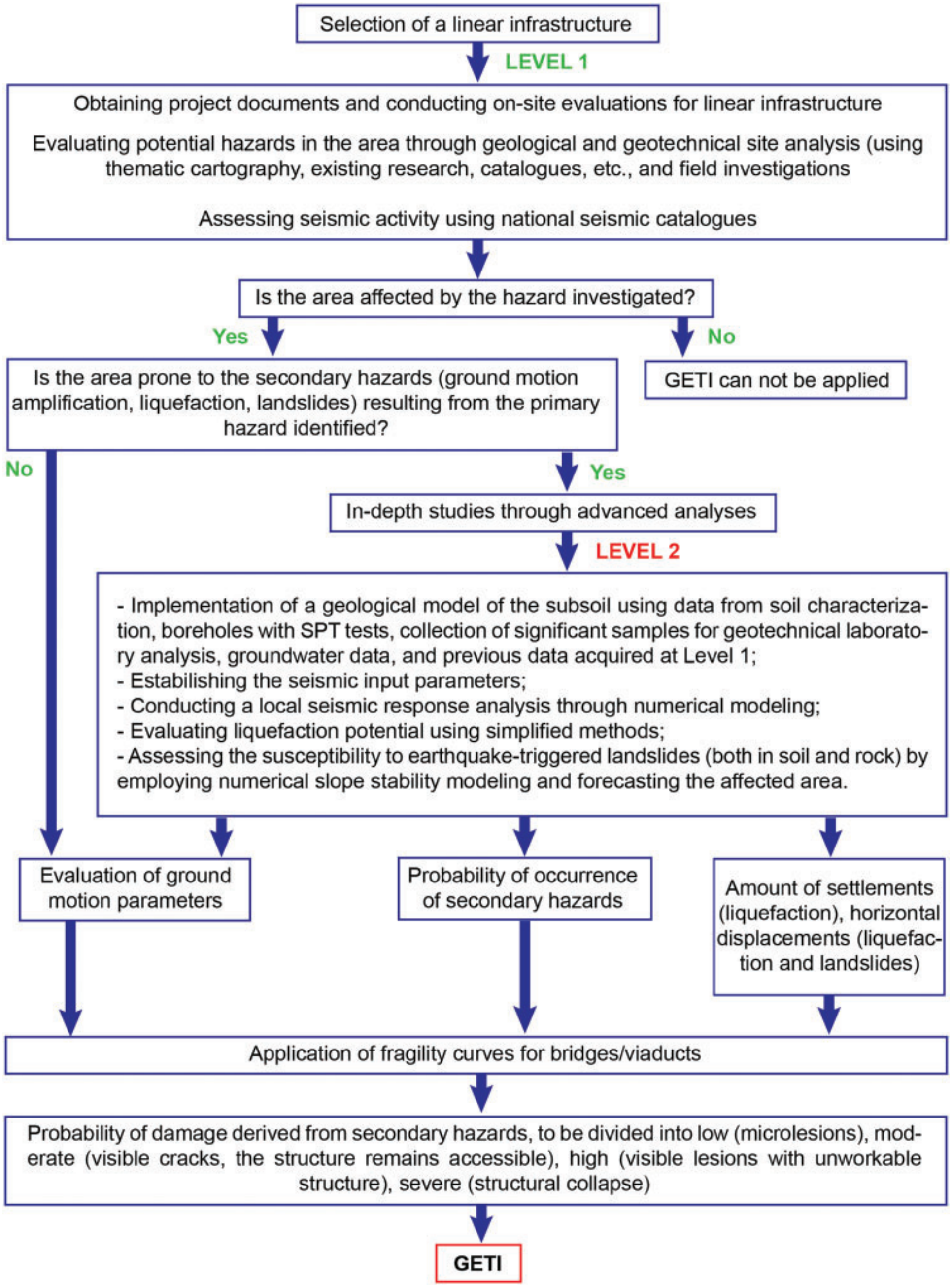

Figure 3. Logic flow of the GETI index considering only its application to seismic risk assessment

maps, and other relevant documents. This review aims to identify the potential hazards that threaten the area under consideration. If the study area is not sufficiently covered by previous studies, reports, or maps, it is mandatory to acquire data from field surveys, using remote sensing, in situ tests, and everything is available and sustainable in terms of costs to characterize the area.

Once it has been ascertained that the studied area is prone to the occurrence of an earthquake (the primary hazard), the subsequent step is to analyze susceptibility to its secondary effects: ground motion amplification (site response), soil liquefaction, and landslide/rockfall occurrence.

As a primary screening method, it is advantageous to employ screening analysis using shake maps to identify the occurrence of ground motion amplification effects, geological-geotechnical criteria to analyze susceptibility to liquefaction, and magnitude-distance and geomorphological-geotechnical criteria to determine susceptibility to landslide/rockfall.

At Level 1, geotechnical tests and laboratory analyses are not required. However, it is essential to conduct surveys to compare the data from the literature with the actual conditions of the area.

The output data should evaluate potential susceptibility to the considered hazards without estimating the probability of their occurrence. If the area is susceptible to one or more hazards, it is necessary to proceed to Level 2 analyses.

Level 2—Advanced analyses

When susceptibility to certain hazards (and their secondary effects) is ascertained, a further step is necessary to determine their probability of occurrence and potential effects on the subsoil and at the surface. From this perspective, acquiring geological and geotechnical data is essential for analyzing hazards using simplified and more advanced (numerical modeling) methods.

Boreholes should be drilled considering the geological framework reconstructed at Level 1 to better understand the stratigraphic asset at the scale of the infrastructure. They also allow for acquiring soil samples for geotechnical characterization through laboratory analyses (e.g., classification and mechanical tests). Moreover, it is important to perform geophysical tests, such as down/cross-hole or multichannel analysis of surface waves, to obtain the shear-wave velocity (V_S) profile with depth at multiple verticals of the subsoil volume affecting the behavior and stability of the bridge/viaduct. The aim is to obtain a robust and detailed model of the subsoil at the scale of the infrastructure.

Regarding the phenomena of ground shaking, liquefaction, and landslide/rockfall associated with seismic activity, the initial phase of Level 2 comprises a site response analysis, soil liquefaction assessment, and slope stability evaluation.

Site response analysis

Site response analysis can be conducted through one-dimensional (1D) or two-dimensional (2D) numerical modeling (contingent on the surficial and buried morphological characteristics of the area driving the potential bi-dimensional effects on ground motion amplification) utilizing available computational codes, as reported by Pagliaroli.[24] The input parameters for site response analyses (subsoil model including stratigraphy and geotechnical properties of the soil, such as V_S, nonlinear stiffness (G/G_0), and damping curves) can be derived from previous studies identified in Level 1 and new tests conducted in Level 2. Additional seismological parameters (M_W and source-to-site distance) are generally required for the selection of input accelerograms applied at the seismic bedrock. The data output yields a PGA profile with depth and other relevant ground motion parameters (i.e., accelerograms or acceleration response spectra at ground surface/foundation depth) quantifying the seismic action on the structure while taking into account ground motion amplification phenomena (Fig. 4).

Soil liquefaction assessment

The potential of soil to liquefy due to seismic activity can be estimated using simplified methods. The first step is to identify the predominant grain size between sand and gravel to better focus the analysis using methods developed for sandy,[22,25] silty,[22,26] and gravelly[27,28] soils. As input data, this approach requires the expected M_W value, PGA value at the surface (including ground motion amplification), depth of the ground water table (GWT), stratigraphy, and geotechnical properties of the soil. Depending on the simplified method selected for the analysis, the mechanical parameters necessary for the analysis are V_S, standard penetration test blow count (N_{spt}), dynamic penetration test blow count (N_{DPT}), or soil resistance measured by cone penetration test (q_c) values derived from in situ tests.

From this, using simplified methods by, as an example, Zhang et al.[29] and Zhang et al.,[30] settlements and horizontal displacements potentially induced by soil liquefaction of ground can be estimated. The liquefaction assessment is performed at the infrastructure scale (Fig. 5).

Slope stability analyses

Simplified methods can be used to conduct slope stability analyses to assess the probability of landslides or rockfalls induced by seismic activity. Regarding landslides, pseudo-static analysis (in which the effects of an earthquake are represented by constant horizontal and/or vertical accelerations) can be used first to derive the critical acceleration value (a_c), defined as the acceleration required to produce slope instability, which is the product of the critical seismic coefficient (k_c) and the acceleration of gravity (g). Newmark sliding block analysis[31] can then be executed to predict the permanent displacements of slopes subjected to ground motion. In this analysis, a potential landslide is considered equivalent to a rigid block resting on an inclined plane. As an alternative to the Newmark analysis, there are many simplified prediction equations available in the literature[32,33] that link the displacement of the slope to the slope critical acceleration value and to several ground motion parameters representative of ground shaking. These equations were developed based on numerous parametric Newmark analyses (Fig. 6).

In addition, in recent literature are available physically-based probabilistic models and hybrid methods, by coupling data-driven methods, to assess landslide susceptibility.[34–37]

To assess rockfall hazard, it is crucial to conduct a geomechanical/morphological survey for the identification of the rockfall source zones (i.e., detachment niches). After that, simplified approaches or trajectographic numerical simulations are generally required to characterize the potential paths and movement characteristics of falling rocks. The key factors for risk estimation include maximum travel distance, bounce height, and translational velocity of the blocks at the moment of impact.

Numerical simulations of rockfall in three dimensions model the occurrence on a full 3-D slope surface.[38] Various software packages are available to implement these runout analyses.[39] The strength of 3-D models lies in their ability to integrate the shape of rock fragments and topography into the resulting dynamic behavior. Nevertheless, these models are limited by their need for numerous spatially explicit maps and substantial computational power. For this reason, 2D models are the best solution for providing an easy-to-use method to model the phenomenon with sufficient accuracy, using commercial software and a less powerful computer.

From hazard to risk: fragility curves

Upon obtaining the values of the PGA, lateral displacements or rock velocities, and vertical settlements, it is possible to assess the potential damage resulting from the interaction of these hazards with the linear structure using *fragility curves*.[1,40,41] Furthermore, the probability of damage can be ascertained by considering four levels of intensity: low, defined as the presence of minor fissures in the infrastructure without compromising its safety and stability; moderate, characterized by visible cracks in the infrastructure, although it may still be deemed accessible; high, indicating that the infrastructure is no longer accessible; and severe, denoting the complete collapse of the structure.

Fragility curves allow for the assessment of the exceeding of pre-established damage states of a structure in probabilistic terms, through a relationship between an earthquake intensity measure, such as the PGA, and the probability that a specific level of damage is reached or exceeded.[42,43] Several fragility curves for bridges are available in the literature, developed by considering the design of the structure, mode of failure, and the geotechnical parameters that can cause damage. For example, the effects of horizontal movements of the ground (lateral spreading due to soil liquefaction) on highway bridges and viaducts are explored by Branderberg et al.[40] considering six different types of structures.

In this study, fragility curves available from the literature are selected to assess the risk from rockfall[44] and ground shaking,[40] using the translational velocity of the falling blocks at the moment of impact on the piles of the viaduct and the PGA at foundation depth, respectively. Four levels of damage (low, moderate, high, and severe) are proposed for each secondary hazard identified in the selected area, utilizing a minimum of four distinct fragility curves for each type of bridge or viaduct.

Conditional probability and the expression of GETI

To express the concept of the “cascade effect” in mathematical terms, the damage derived, for example, from ground shaking, liquefaction, and landslides, considered as secondary effects of the occurrence of an earthquake, can be described by conditional probability.

Conditional probability can be defined[45] as follows:

$$P(A|B) = \frac{P(A \cap B)}{P(B)} \tag{2}$$

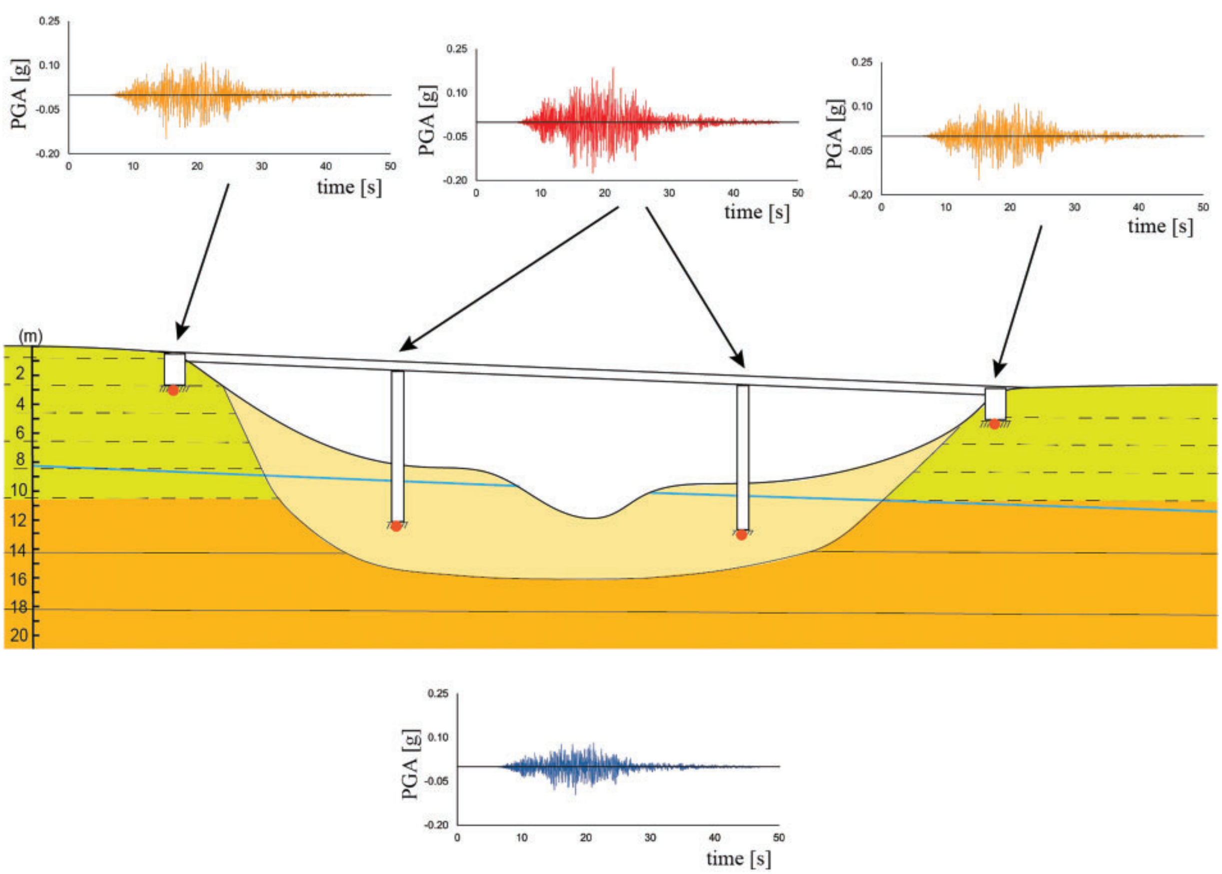

Figure 4. Sketch of a 2D site response analysis of a bridge crossing a valley filled by alluvial soils, showing typical results of ground motion at the foundations level. The blue accelerogram represents the seismic input at bedrock for an assigned seismic scenario (defined by a certain probability of occurrence/return period), while the red and orange accelerograms represent the ground motion at the foundations level. Yellow and orange polygons represent stratified consolidated deposits, while light yellow depicts loose deposits

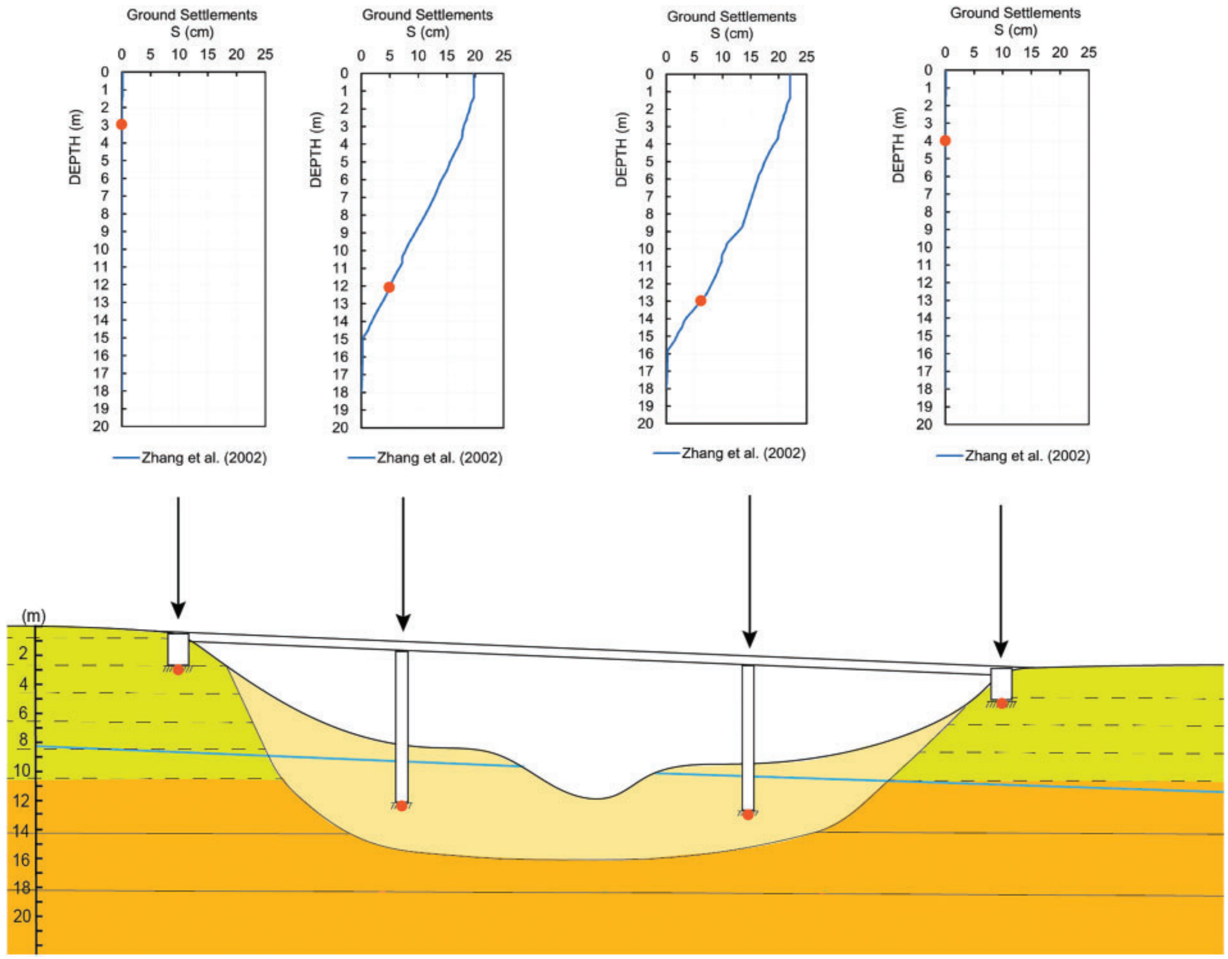

Figure 5. Sketch of a bridge crossing a valley filled by alluvial soils, showing typical results of liquefaction analyses in terms of permanent settlements at foundation levels. Yellow and orange polygons represent stratified consolidated deposits, while light yellow depicts loose deposits. The cumulative ground settlements according to Zhang et al.[29] are plotted; orange circles depict the foundations level; the blue line represents the ground water table

where A is the event whose uncertainty we want to update, and B is the evidence we want to treat as given. We call P(A) the prior probability of A, intended as before updating, and P(A|B) the posterior probability of A, considered after updating based on the evidence.

By moving the denominator in the definition to the other side of the equation, we can obtain that

$$P(A \cap B) = P(B)\, P(A|B) \tag{3}$$

If P(A) > 0 and P(B) > 0, then this is equivalent to P(A|B) = P(A), and also equivalent to P(B|A) = P(B). If events A and B are independent, the above relation can be written as

$$P(A \cap B) = P(A)\, P(B) \tag{4}$$

From this, we can say that two events are independent if we can obtain the probability of their intersection by multiplying their individual probabilities.

If $P(A \cap B) \neq 0$, it is true that they are compatible, so they can occur simultaneously. However, the likelihood of A happening does not influence the likelihood of B happening, or vice versa.

By considering three events A, B, and C, they can be defined as independent if all of the following equations are verified:

$$P(A \cap B) = P(A)\, P(B) \tag{5a}$$

$$P(A \cap C) = P(A)\, P(C) \tag{5b}$$

$$P(B \cap C) = P(B)\, P(C) \tag{5c}$$

$$P(A \cap B \cap C) = P(A)\, P(B)\, P(C) \tag{5d}$$

From this, it is possible to shift to natural hazards, specifically examining the occurrence of an earthquake (E). In this case, there can be three related events: ground shaking (with or without ground motion amplification), liquefaction (also intended as lateral spreading), and landslide/rockfall that could affect the linear infrastructure.

The surficial effects of an earthquake are strictly related to the PGA value, which can be determined using risk maps (probabilistic scenario) followed by LSR. Upon obtaining the values of PGA, impact velocity, lateral displacements, and vertical settlements, it is possible to assess the potential damage resulting from the interaction of these hazards with the linear structure using fragility curves, obtaining $P(D|S)$,

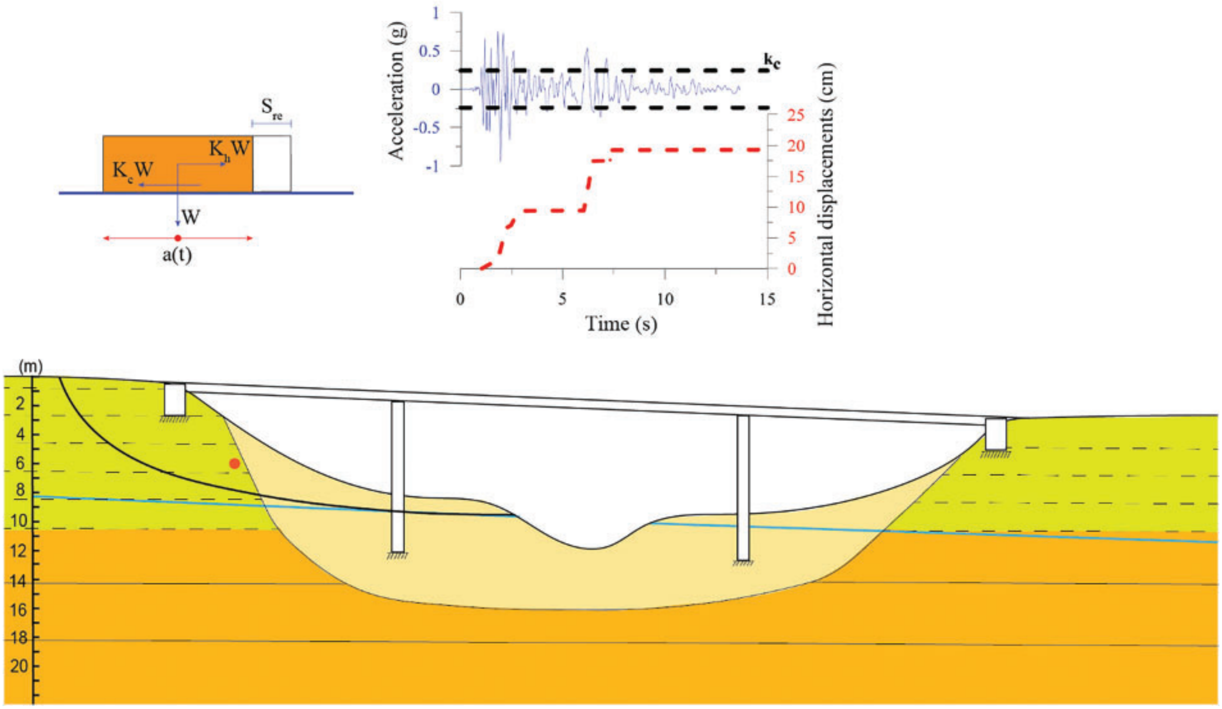

Figure 6. Sketch of a bridge crossing a valley filled by alluvial soils showing typical results of Newmark slope analyses in terms of permanent displacements. The accelerogram a(t) is computed at the center of mass (orange point) of the potential landslide. k_c is the critical seismic coefficient (dashed blue line), W is the weight of the block corresponding to the unstable mass, and S_{re} is the horizontal permanent displacement of the unstable mass at the end of the shaking. Yellow and orange polygons represent stratified consolidated deposits, while light yellow depicts loose deposits and the black curve identifies the detachment surface

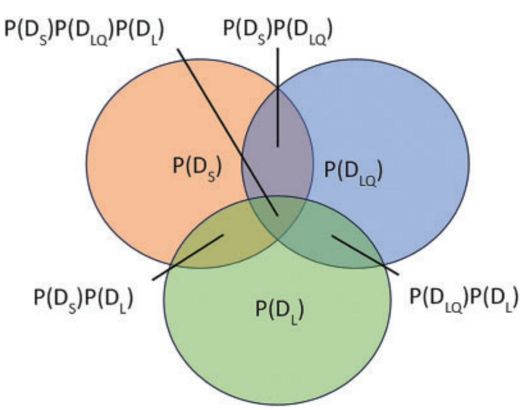

Figure 7. Visual representation of the sum of $P(D_S)$, $P(D_{LQ})$, and $P(D_L)$, intended as the whole area covered by the three circles

$P(D|LQ)$, $P(D|L)$. To prevent complicated writing, it isexpressed as follows:

$$P(D|S) = P(D_S) \tag{6a}$$

$$P(D|LQ) = P(D_{LQ}) \tag{6b}$$

$$P(D|L) = P(D_L) \tag{6c}$$

These three phenomena can be considered to be acting simultaneously on the infrastructure, so the occurrence of one does not influence the damage resulting from another. Considering the above equations and definitions, these three events are independent, and it is possible to express their intersection by multiplying their probabilities:

$$P(D_S \cap D_{LQ}) = P(D_S)\,P(D_{LQ}) \tag{7a}$$

$$P(D_S \cap D_L) = P(D_S)\,P(D_L) \tag{7b}$$

$$P(D_{LQ} \cap D_L) = P(D_{LQ})\,P(D_L) \tag{7c}$$

$$P(D_S \cap D_{LQ} \cap D_L) = P(D_S)\,P(D_{LQ})\,P(D_L) \tag{7d}$$

The following diagram depicts the meaning of these equations:

As it is possible to see, the total probability of damage is given by the sum of the probability of occurrence of damages derived from ground shaking $P(D_S)$, liquefaction $P(D_{LQ})$, and landslide/rockfall $P(D_L)$, subtracting the areas of overlap, obtaining:

$$\begin{aligned} P(D_T) = {} & P(D_S) + P(D_{LQ}) + P(D_L) - P(D_S)\,P(D_{LQ}) \\ & - P(D_S)\,P(D_L) - P(D_{LQ})\,P(D_L) \\ & + P(D_S)\,P(D_{LQ})\,P(D_L) \end{aligned} \tag{8}$$

Consequently, the GETI index can be expressed as the total probability of damage potentially derived from the occurrence of ground shaking, soil liquefaction, and landslides, calculated for each considered class of damage:

$$GETI_L = P(D_{SL}) + P(D_{LQ_L}) + P(D_{LL})$$

$$- P(D_{SL}) P(D_{LQ_L}) - P(D_{SL}) P(D_{LL}) - P(D_{LQ_L}) P(D_{LL}) + P(D_{SL}) P(D_{LQ_L}) P(D_{LL}) \tag{9a}$$

$$GETI_M = P(D_{SM}) + P(D_{LQ_M}) + P(D_{LM}) - P(D_{SM}) P(D_{LQ_M}) - P(D_{SM}) P(D_{LM}) - P(D_{LQ_M}) P(D_{LM}) + P(D_{SM}) P(D_{LQ_M}) P(D_{LM}) \tag{9b}$$

$$GETI_H = P(D_{SH}) + P(D_{LQ_H}) + P(D_{LH}) - P(D_{SH}) P(D_{LQ_H}) - P(D_{SH}) P(D_{LH}) - P(D_{LQ_H}) P(D_{LH}) + P(D_{SH}) P(D_{LQ_H}) P(D_{LH}) \tag{9c}$$

$$GETI_S = P(D_{SS}) + P(D_{LQ_S}) + P(D_{LS}) - P(D_{SS}) P(D_{LQ_S}) - P(D_{SS}) P(D_{LS}) - P(D_{LQ_S}) P(D_{LS}) + P(D_{SS}) P(D_{LQ_S}) P(D_{LS}) \tag{9d}$$

where $GETI_L$ is the probability of low damage; $GETI_M$ is the probability of moderate damage; $GETI_H$ is the probability of high damage; and $GETI_S$ is the probability of severe damage. Parameters $GETI_L$, $GETI_M$, $GETI_H$, and $GETI_S$ can be calculated using the Eqs. (9a)–(9d), which are derived from fragility curves developed for low, moderate, high, and severe damage, respectively, and for the three secondary hazards considered in this study.

Application of Geti: The Case Study of Central Italy

To assess the applicability and practical efficacy of the index, GETI was applied to a case study in Italy. The objective of this empirical application is to evaluate whether the proposed procedure can yield the anticipated results, determine its degree of accuracy and precision, and ascertain its potential as a tool for managers to assess the safety of linear infrastructure, such as bridges and road viaducts.

The selected viaduct is situated in the Abruzzo Region (Central Italy), a region characterized by an active extensional tectonic phase, as evidenced by several significant earthquakes over the past two centuries.[46] Furthermore, the viaduct is located in proximity to a fault system considered active and capable.[47,48]

The viaduct is situated in close proximity to the eastern slope of a carbonate relief, which is susceptible to rockfall,[48] as documented in the Level 1 Seismic Microzonation studies. Furthermore, the viaduct is constructed upon lacustrine sediments interspersed with material derived from the slope, rendering it potentially susceptible to ground motion amplification and liquefaction.

Given these considerations, the viaduct was selected as a case study for the application of the GETI index. In accordance with the logical framework presented in Fig. 3, the initial step involved the acquisition of the viaduct design and construction documents, geological maps, seismic microzonation studies, and all available geological and geotechnical literature data pertaining to the selected area.

Level 1: Structural framework

The viaduct was constructed from 1991 to 2001, with a length of 343 m and comprising 10 spans of 35 m each. It features a Gerber truss configuration and 9 piles for each track, in addition to abutments. The track partially overlooks a developed area and follows a straight alignment compliant with the main extra-urban road of type B. The road platform consists of two independent tracks, each approximately 7 m wide, accommodating two unidirectional lanes and the right-hand paved quay, without grade intersections, and equipped with a restraint curb on both sides.

The viaduct's structural design incorporates prefabricated prestressed concrete Gerber beams with post-tensioned cables and a continuous slab, decoupled stem batteries cast in situ, and monolithic reinforced concrete abutments. The observed access points to the viaduct are constructed of soil. The piles and abutments of the viaduct are supported by shallow foundations positioned 3 m below ground level. The foundation soil was reinforced using micropiles extending to a depth of 15 m.

Level 1: Geological framework

The viaduct is situated in Quaternary intermontane extensional basins in the Central Apennines (Italy). The basin exhibits a half-graben geometry, resulting from the activity of two primary normal and right-lateral strike-slip fault systems. Paleoseismological investigations of this fault system have revealed the occurrence of at least 10 paleoearthquakes in the past 33 ky, with a recurrence interval ranging from 1400 to 2600 years.[47,48]

The basin, predominantly composed of lacustrine sediments, is superimposed on Mesozoic to Tertiary carbonates and syn-orogenic flysch rocks,[48] and it is bordered by mountains consisting of deeply fractured Meso-Cenozoic carbonates. The viaduct is positioned in proximity to the slope, in an area that has been subject to rockfall events in the past, as documented in seismic microzonation studies. The occurrence of such events is further corroborated by observations of rockfall deposits in the stratigraphic logs from seven boreholes drilled during the initial phase of viaduct construction (Fig. 8).

Level 1: Data analysis and conclusions

Considering the first part of the logic flow of the GETI index (Fig. 3), the question to address is, "Is the area affected by the hazard investigated?" Based on data acquired from literature and geological/geotechnical surveys, it is possible to conclude that the viaduct is exposed to seismic hazard due to the presence of an active fault system in the near field. The proximity of the structure to the mountain slope and the structural features of the rock mass make the viaduct potentially susceptible to rockfall hazard, while the presence of an approximately 40-m-thick lacustrine deposit beneath the foundation may induce ground motion amplification phenomena.

It appears feasible to exclude the occurrence of soil liquefaction due to the absence of a water table in the first 20

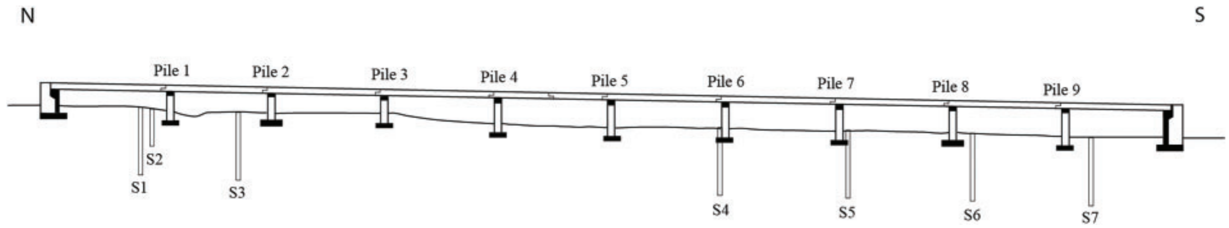

Figure 8. Schematic longitudinal section view of the boreholes drilled under the viaduct. The stratigraphic logs show coarse material mixed with lacustrine fine sediments in the first 12–13 m, overlaying lacustrine deposits

m below the ground surface. Furthermore, the stratigraphic logs indicate the presence of approximately 10 m of very coarse slope material, which is typically not susceptible to liquefaction.

Consequently, comprehensive studies are necessary for risk assessment and to accurately apply the GETI index.

Level 2: Site response analysis

To analyze the potential for ground motion amplification and quantify the PGA value corresponding to the foundation soil deposit of the viaduct, a site response analysis was conducted using the 1D nonlinear time domain DEEPSOIL code version 7.1.[49] Given the relevance of the viaduct, a design reference period of 75 years was assumed, and consequently, a 712-year return period scenario was selected based on the Italian seismic code (NTC, 2018) for Ultimate Limit State (SLV). Utilizing the probabilistic seismic hazard assessment of Italy from Istituto Nazionale di Geofisica e Vulcanologia studies[50] and implemented in NTC2018, an a_g value of 0.28 g can be assumed as the acceleration input at the seismic bedrock.

Seven natural accelerograms were selected in accordance with the seismological characteristics (expected magnitude and source-to-site distance of the regional fault systems), and scaled to the considered a_g value. Subsequently, the seismic input was applied at the seismic bedrock (characterized by $V_S = 1200$ m/s) located at a depth of 40 m as deduced from data from previous studies.

Above the bedrock, the stratigraphy of the area beneath the viaduct is variable and affected by coarse and chaotic material, likely derived from rockfall and/or erosion in the first 12 m below ground level. The ground motion amplification effects were modeled through site response analyses based on seven stratigraphic logs available from previous studies and considered representative of geological and geotechnical conditions along the viaduct.

In this regard, and considering the position of the piles in relation to the slope, the stratigraphy of boreholes S4, S5, S6, and S7, corresponding to piles from 6 to 9, and to the southern abutment, was extended to piles from 3 to 5. The stratigraphy of boreholes S1, S2 and S3 was considered for the abutment in the northern part of the structure, as well as for the first two piles (Fig. 8). The Vs profiles of the models adopted in the analyses are shown in Fig. 9a. The effect of micropile improvement in the upper 15 m of subsoil was not considered in the analysis. As a result, seven PGA profiles were obtained (Fig. 9b).

To determine the behavior of the structure under the action of the earthquake, an average value of PGA was calculated using the seven profiles, obtaining a PGA value at the foundation level (3 m below the ground surface) of 0.34 g.

Level 2: Rockfall assessment

Previous studies[48] conducted on the slope in question revealed strata dipping in the slope direction and that the rock mass is also affected by several families of persistent fractures perpendicular to the stratum boundaries. Analyses based on the limit equilibrium method (pseudo-static approach) conducted on the same slope indicate a minimum threshold of 0.09 g for block slip.[51] Considering that peak accelerations reach values about 3 times higher than the threshold, the detachment of blocks from the slope in the event of an earthquake is considered highly probable.

To quantify the probability of the interaction between rockfall and the structure and determine the impact velocity, a numerical model was created using Rockfall2D code by Rocscience Inc. As input data, nine profiles derived from a Digital Terrain Model (DTM) with 1 m resolution (http://wms.pcn.minambiente.it) were traced in correspondence of six piles and the two abutments of the viaduct, considering the maximum slope value for each. The nine 2D models of the slope were utilized to model the occurrence of rockfall, considering as seeders the scarps or discontinuities of the slope shape.

The position of each individual pile in each profile was estimated from DTM, satellite, and survey data, and the velocity of the rocks' impact on the pile was calculated considering the estimated velocity of the blocks when they reach this position on the profile (Fig. 10).

Based on data from seismic microzonation studies and from Di Naccio et al.,[48] three diameters of blocks of 1.2, 1.5, and 1.8 m, with spherical shape, were considered. The block sizes are comparable with the fragility curves proposed by Xie et al.[44].

As a result, 100% of the rocks impacted pile 1 west and 25% were able to impact pile 1 east, with an average velocity of approximately 17 m/s. Pile 2 west was impacted by 10% of the blocks with an average velocity of 15 m/s, while piles from 3 to 9 were not impacted by rocks in this simulation.

Level 2: Fragility curves

The results from site response and rockfall analyses are used as input parameters in the fragility curves developed by

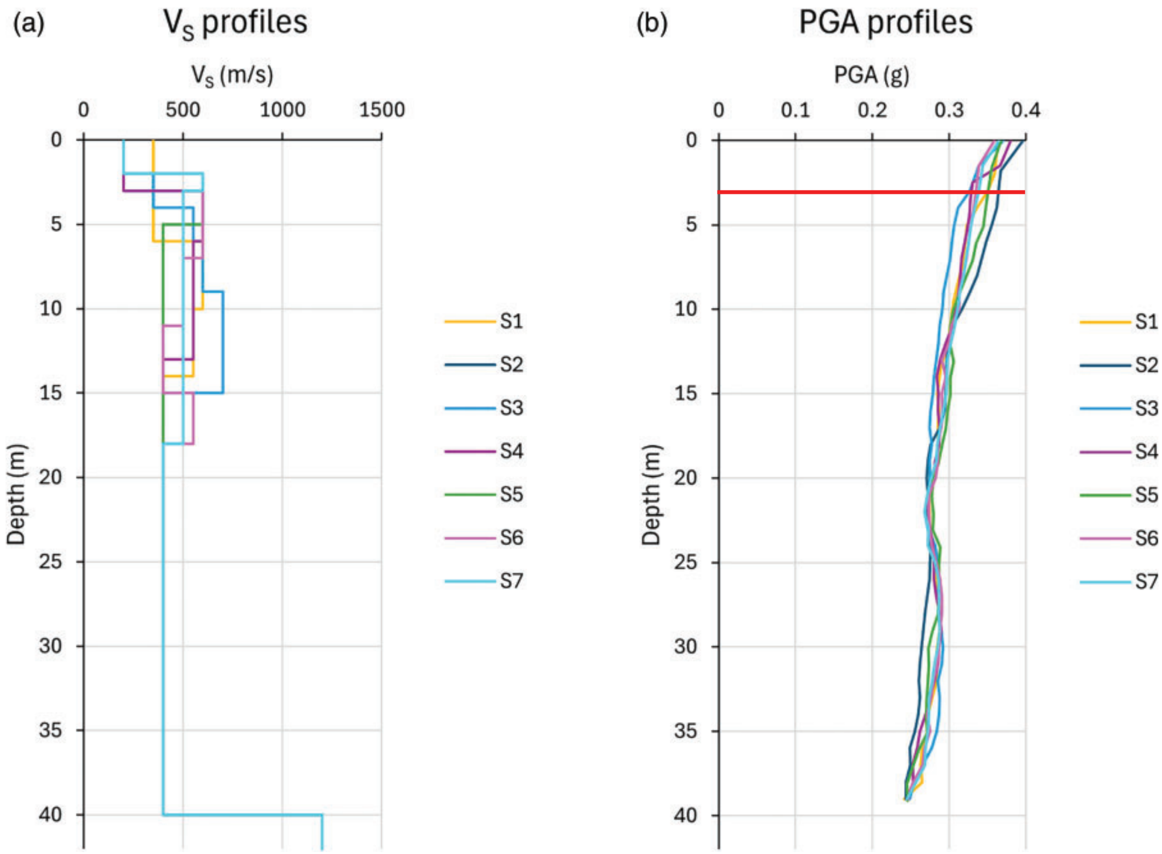

Figure 9. (a) V_S profiles deducted from microzonation studies and adopted for site response analyses; (b) PGA profiles, considering boreholes S1, S2, S3, S4, S5, S6, and S7, obtained through the site response analysis using DEEPSOIL code version 7.1.[49] The red line represents the foundation level

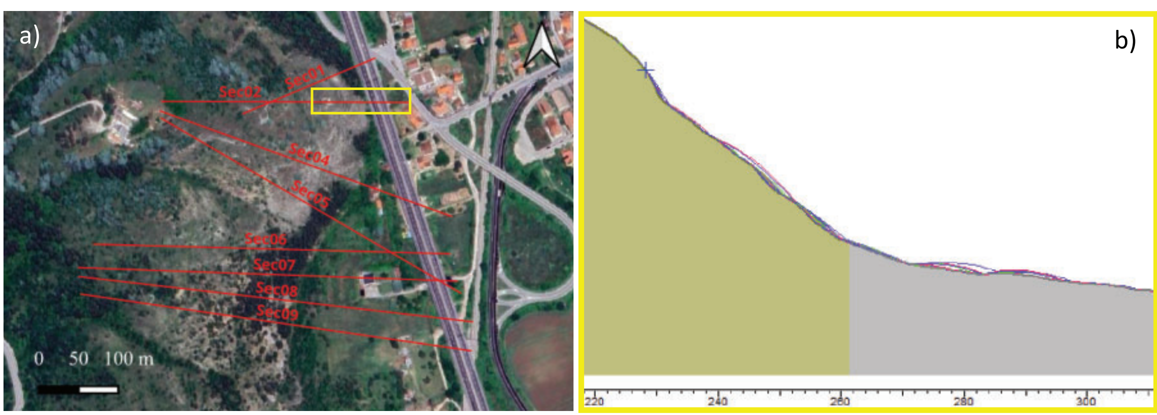

Figure 10. (a) Satellite (Google Earth) view of the slope near the viaduct; red lines depict the section traces, and the yellow box indicates the slope profile reported in (b). (b) Slope profile with detachment points (crosses) and trajectories (red and blue lines) of falling blocks, as simulated using the Rockfall2D code

Brandenberg et al.[40] and Xie et al.[44] for the consequences of seismic ground shaking and rock impact velocity, respectively (Fig. 11).

Regarding the fragility curves proposed by Brandenberg et al.,[40] those for bridge type E5 (seat abutment and continuous with expansion joint and pier isolation), corresponding to the bridge under study, were used to determine the probability of damage for the selected viaduct.

In addition, it is essential to emphasize that the viaduct comprises two semi-independent tracks with common abutments; each track has nine piles. In this context, the state of collapse is defined as the loss of functionality of both tracks due to the rupture of two piles during the rockfall. As the viaduct presents an isostatic scheme, the impact of rocks on one pile is considered sufficient to cause damage to the structure; consequently, the higher velocity together with the higher percentage of impacting blocks were used

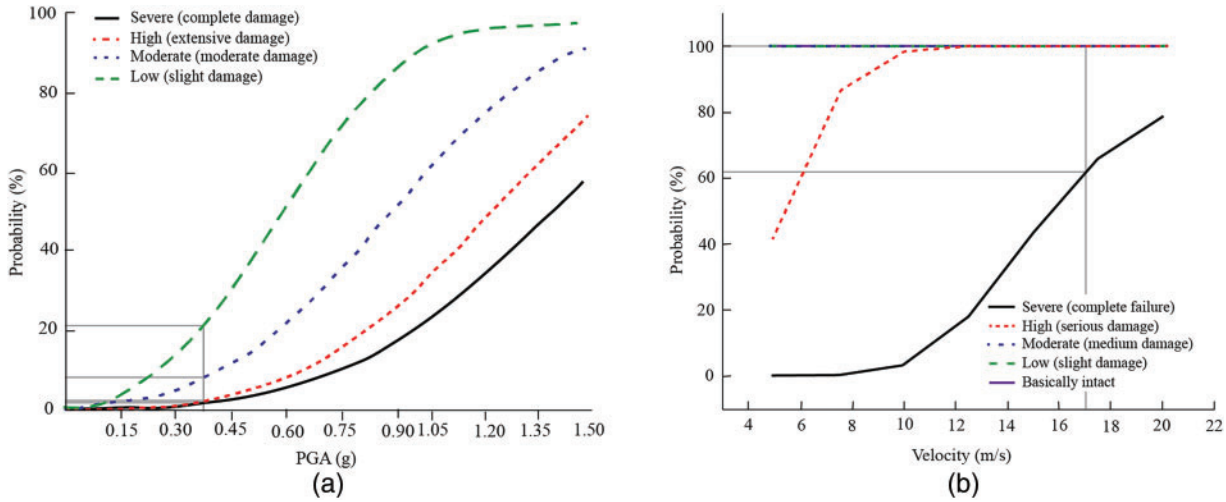

Figure 11. Fragility curves for damage on bridges derived from (a) ground shaking (modified from Brandenberg et al.[40]) and (b) rockfall (modified from Xie et al.[44]). Gray lines represent PGA and block impact velocity resulting from the analyses conducted in this study

as parameters in damage determination. Thus, considering that 100% of rocks impact pile 1 west, but only 25% of the blocks impact pile 1 east, potentially causing the collapse of the entire structure, the resulting probability of damage is defined by Eq. (3) as the product of the probability of damage due to the rocks' impact and the probability of impact as the percentage of rock blocks that reach the eastern pile.

It should be considered that the employed fragility curves adopt square piles, while in the case study, the piles are rectangular in shape, which may lead to conservative results.

The results in terms of damage probability for the three seismic phenomena (shaking, liquefaction, and rockfall) are shown in Table 1. If liquefaction is obviously zero as stated in Level 1 assessment, the most important contribution to damage is related to rockfall for all damage classes while ground shaking (even considering amplification effects) plays a less relevant role. Intervention strategies for seismic risk mitigation of the viaduct should therefore focus on rockfall, i.e., protection of the viaduct from block impact (rockfall barriers) or consolidation of the slope to prevent the detachment of rock blocks.

Table 1. Probability of damage derived from fragility curves for low, medium, high, and severe damage referred to, respectively, ground shaking, soil liquefaction, and landslide/rockfall

	$P(D_S)$	$P(D_{LQ})$	$P(D_L)$
Low	0.22	0	0.25
Medium	0.08	0	0.25
High	0.04	0	0.25
Severe	0.03	0	0.16

Level 2: Computing

Following the determination of probabilities for low, moderate, high, and severe damage, the GETI was calculated using Eqs. (9a)–(9d).

Subsequently, the GETI was derived as follows:

$$\begin{aligned}\boldsymbol{GETI_L} &= 0.22 + 0 + 0.25 - 0.22 * 0 - 0.22 * 0.25 \\ &\quad - 0 * 0.25 + 0.22 * 0 * 0.25 = 0.415 = \mathbf{41\%}\end{aligned}$$

$$\begin{aligned}\boldsymbol{GETI_M} &= 0.08 + 0 + 0.25 - 0.08 * 0 - 0.08 * 0.25 \\ &\quad - 0 * 0.08 + 0.08 * 0 * 0.25 = 0.31 = \mathbf{31\%}\end{aligned}$$

$$\begin{aligned}\boldsymbol{GETI_H} &= 0.04 + 0 + 0.25 - 0.04 * 0 - 0.04 * 0.25 \\ &\quad - 0 * 0.25 + 0.04 * 0 * 0.25 = 0.28 = \mathbf{28\%}\end{aligned}$$

$$\begin{aligned}\boldsymbol{GETI_S} &= 0.03 + 0 + 0.16 - 0.03 * 0 - 0.03 * 0.16 \\ &\quad - 0 * 0.16 + 0.03 * 0 * 0.16 = 0.185 = \mathbf{18\%}\end{aligned}$$

Conclusions

In short, the GETI index is proposed as an easy-to-use instrument for risk assessment from a multi-hazard perspective, applied to linear infrastructure such as road bridges and viaducts. The index is conceptualized as a two-level analysis process, using geotechnical parameters to assess the risk through fragility curves. The output data are the probabilities of low, moderate, high, and severe damage, given the earthquake and its secondary effects.

The effectiveness of the GETI is contingent upon the availability and accuracy of the historical and geological hazard data. Spatial and temporal variabilities in hazard occurrence and impact could limit the applicability and accuracy of the index, necessitating continuous updates and regional calibrations to maintain its relevance and reliability.

The precision of the GETI is highly dependent on the quality and completeness of the underlying data. In regions where geological and geotechnical data are scarce or outdated, the accuracy of the risk assessment can be compromised. Efforts to standardize the data collection and encourage the sharing of geotechnical information can mitigate this limitation, as well as the use of technologies like remote sensing.

To assess the applicability and practical efficacy of the index, GETI was applied to a case study in Italy consisting of a viaduct subject to significant shaking and rock block impact due to rockfall phenomena. GETI Level 2 analyses consisted of site response analyses to quantify the seismic actions on the viaduct and runout numerical analyses to assess block velocity impact at the piles. The application of GETI revealed that the most relevant hazard is related to rockfall. This application highlights that GETI may help stakeholders prioritize mitigation actions, optimizing costs and time.

Although the current formulation of the GETI index, limited to assessing seismic risk to linear infrastructure, takes into account the "cascade effect," it overlooks complex interactions between different types of hazards and their secondary effects. In fact, this focus omits the assessment of other critical hazards, such as hydrological, atmospheric, and fire-related events, which pose significant risks to linear infrastructure. Future iterations of the GETI index should aim to include a broader spectrum of natural hazards. This expansion would cover a wider range of potential risks to linear infrastructure, enhancing the comprehensiveness and applicability of the index.

Furthermore, future research should aim to extend the applicability of the index to other linear infrastructure, such as railways and pipelines, and to other types of structures, such as buildings. The GETI can also be used to strategically implement interventions on structures facing the highest risk in an efficient manner.

Acknowledegments

This research activity is part of a PhD thesis under the National Doctoral Course in Defense Against Natural Risks and Ecological Transition of Built Environment. The authors would like to thank FABRE–"Research consortium for the evaluation and monitoring of bridges, viaducts, and other structures" (www.consorziofabre.it/en) for the data and experience acquired during the activities of the FABRE-ANAS 2021-2024 research program.
Special thanks to Prof. Kyle Rollins of Brigham Young University in Provo and Dr. Valerio Piattelli of the University of Chieti-Pescara for their invaluable support in reviewing the theoretical formulation of GETI.

References

[1] Hwang H, Liu JB, Chiu YH. Seismic fragility analysis of highway bridges. In: *Mid-America Earthquake Center Technical Report–MAEC RR-4 Project*. TN 38152, US: Center of Earthquake Research and Information-University of Memphis; 2001:127.

[2] Western J, Bye P, Valeo M, Thompson PD, Frazier E. Assessing risk for bridge management–final report. In: *AASHTO Standing Committee on Highways–National Cooperative Research Program Project 20-7 Task 378*. 2016:121. http://apps.trb.org/cmsfeed/TRBNetProjectDisplay.asp?ProjectID=3924.

[3] MIMS. Linee Guida per la Classificazione e Gestione del Rischio, la Valutazione della Sicurezza ed il Monitoraggio dei Ponti Esistenti. Gazzetta Ufficiale n. 196; D.M. 204 del 1 Luglio 2022. https://www.gazzettaufficiale.it/eli/id/2022/08/23/22A04700/sg.

[4] FEMA. *National Risk Index Technical Documentation*. U.S. Department of Homeland Security, United States of America; 2023. https://www.fema.gov/flood-maps/products-tools/national-risk-index.

[5] Hewitt K, Burton I. *The Hazardousness of a Place: a Regional Ecology of Damaging Events*. Toronto, ON, Canada: University of Toronto Press; 1971:84.

[6] UNCED. Agenda 21. *United Nations Conference on Environment & Development*. Rio de Janeiro, Brazil; June 3 to 14, 1992.

[7] Kappes MS. *Multi-Hazard Risk Analyses: A Concept and Its Implementation*. PhD Thesis. Vien University; 2011.

[8] Greiving S, Fleischhauer M, Luckenkotter J. A methodology for an integrated risk assessment of spatially relevant hazards. *J Environ Plan Manage*. 2006;49(1):1–19. doi:10.1080/09640560500372800.

[9] Zaghi AE, Padgett JE, Bruneau M, et al. Characterizing the problem, and identifying future opportunities in multi-hazard design. *J Struct Eng*. 2016;142(12):86. doi:10.1061/(ASCE)ST.1943-541X.0001586.

[10] Gill JC, Malamud BD. Reviewing and visualing the interactions of natural hazards. *Rev Geophys*. 2014;52:680–722. doi:10.1002/2013RG000445.

[11] Salvatore W, Uva G, Venenzi I, et al. Application of Italian Guidelines for structural-foundational and seismic risk classification of bridges: the Fabre experience on a large bridge inventory. *Procedia Struct Integ*. 2024;62:1–8. doi:10.1016/j.prostr.2024.09.009.

[12] NTC. Aggiornamento delle "Norme tecniche per le costruzioni". D.M. 17 gennaio 2018, pubblicato sul Supplemento ordinario alla Gazzetta Ufficiale, n.42 del 20 febbraio 2018, Serie generale, pp. 372.

[13] Zuzak C, Mowrer M, Goodenough E, Burns J, Ranalli N, Rozelle J. The national risk index: establishing a nationwide baseline for natural hazard in the US. *Nat Hazards*. 2022;114:2331–2355. doi:10.1007/s11069-022-05474-w.

[14] Kappes MS, Papathoma-Köhle M, Keiler M. Assessing physical vulnerability for multi-hazards using an indicator-based methodology. *Appl Geograp*. 2012;32:577–590.

[15] CSRS16. *Infrastrutture: focus con Anas sul ponte di Rotella. Commissario Straordinario Ricostruzione Sisma 2016*. Presidenza del Consiglio dei Ministri; 2023. https://sisma2016.gov.it/2023/09/05/infrastrutture-focus-con-anas-sul-ponte-di-rotella/.

[16] IRPI. *Frane e fenomeni alluvionali in Italia settentrionale. Istituto di Ricerca per la Protezione Idrogeologica (IRPI)*. Consiglio Nazionale delle Ricerche (CNR); 2023. https://polaris.irpi.cnr.it/frane-e-fenomeni-alluvionali-in-italia-settentrionale/.

[17] Odeh JD. Natural hazards vulnerability assessment for statewide mitigation planning in Rhode Island. *Nat*

Hazards Rev. 2002;3(4):177–187. doi:10.1061/(ASCE)1527-6988(2002)3:4(177).

[18] Dilley M, Chen RS, Deichmann U, Lerner-Lam AL, Arnold M. Natural disaster hotspots–a global risk analysis. In: *Disaster Risk Management Series*. Washington, DC: World Bank; 2005. license:CC BY 3.0 IGO. http://hdl.handle.net/10986/7376.

[19] ICPD. *National Risk Assessment–Overview of the Potential Major Disasters in Italy: Seismic, Volcanic, Tsunami, Hydro-Geological/Hydraulic and Extreme Weather, Droughts and Forest Fire Risk*. Italian Civil Protection Department (ICDP); 2018:137. https://www.protezionecivile.gov.it/static/5cffeb32c9803b0bddce533947555cf1/Documento_sulla_Valutazione_nazionale_dei_rischi.pdf.

[20] Fiore A, Ottaviani V. Rischio sismico in Italia: analisi e prospettive per una prevenzione efficace in un Paese fragile. *Supplemento a Geologia dell'Ambiente, SIGEA*. 2018:1.

[21] Schnabel P, Bolton Seed H, Lysmer J. Modification of seismograph records for effects of local soil conditions. *Bull Seismol Soc Am*. 1972;62(6):1649–1664. doi:10.1785/BSSA0620061649.

[22] Idriss IM, Boulanger RW. *Soil liquefaction during earthquakes*. Oakland, California, USA: Earthquake Engineering Research Institute (EERI). 2008:237.

[23] Keefer DK. Landslides caused by earthquakes. *GSA Bull*. 1984;95(4):406–421. doi:10.1130/0016-760695<406:LCBE>(1984)2.0.CO;2.

[24] Pagliaroli A. Key issues in Seismic Microzonation studies: lessons from recent experiences in Italy. *Rivista Italiana di Geotecnica*. 2018;1:6–48. doi:10.19199/2018.1.0557-1405.005.

[25] Andrus RD, Stokoe KH. Liquefaction resistance of soils from shear-wave velocity. *J Geotech Geonviron Eng*. 2000;126(11):1015–1025.

[26] Andrews CA, Martin GR. Criteria for liquefaction of silty soils. *Proceedings of the 12th World Conference in Earthquake Engineering*; 2000; Auckland, New Zeland.

[27] Rollins KM, Roy J, Athanasopoulos-Zekkos A, Zekkos D, Amoroso S, Cao Z. A new dynamic cone penetration test-based liquefaction triggering assessment of gravelly soils. *J Geotech Geoenviron Eng*. 2021;147(12):04021141. doi:10.1061/(ASCE)GT.1943-5606.0002686.

[28] Rollins KM, Roy J, Athanasopoulos-Zekkos A, Zekkos D, Amoroso S, Cao Z, Milana G, Vassallo M, Di Giulio G. A new VS-based liquefaction-triggering procedure for gravelly soils. *J Geotech Geoenviron Eng*. 2022;148(6):04022040. doi:10.1061/(ASCE)GT.1943-5606.0002784.

[29] Zhang G, Robertson PK, Brachman RWI. Estimating liquefaction-induced ground settlements from CPT for level ground. *Canadian Geotech J*. 2002;39:1168–1180. doi:10.1139/t02-047.

[30] Zhang G, Robertson PK, Brachman RWI. Estimating liquefaction-induced lateral displacements using the standard penetration test or cone penetration test. *J Geotech Geoenviron Eng*. 2004;130(8):861–871. doi:10.1061/(ASCE)1090-0241(2004)130:8(861).

[31] Newmark NM. Effects of earthquakes on dams and embankments. *Geotechnique*. 1965;15(2):139–160. doi:10.1680/geot.1965.15.2.139.

[32] Whitman RV, Liao S. Seismic design of gravity retaining walls. *Proceding 8th World Conference on Earthquake Engineering*; 1984; San Francisco.

[33] Crespellani T, Madiai C, Vannucchi G. Earthquake destructiveness potential factor and slope stability. *Géotechnique*. 1998;48(3):411–419.

[34] Ji J, Cui H, Zhang T, Song J, Gao Y. A GIS-based tool for probabilistic physical modelling and prediction of landslides: GIS-FORM landslide susceptibility analysis in seismic areas. *Landslides*. 2022;19:2213–2231. doi:10.1007/s10346-022-01885-9.

[35] Pei T, Qiu T. Landslide susceptibility mapping using physics-guided machine learning: a case study of a debris flow event in Colorado Front Range. *Acta Geotechnica*. 2024;19:6617–6641. doi:10.1007/s11440-024-02384-y.

[36] Montrasio L, Gatto MPA, Miodini C. The role of plants in the prevention of soil-slip: the G-SLIP model and its application on territorial scale through G-XSLIP platform. *Landslides*. 2023;20:1149–1165. doi:10.1007/s10346-023-02031-9.

[37] Gatto MPA, Lentini V, Montrasio L, Castelli F. A simplified semi-quantitive procedure based on the SLIP model for landslide risk assessment: the case study of Gioiosa Marea (Sicily, Italy). *Landslides*. 2023;20:1381–1403. doi:10.1007/s10346-023-02040-8.

[38] Descoeudres F, Zimmermann T. Three-dimensional dynamic calculation of rockfalls. In: *Sixth International Congress on Rock Mechanics. International Society for Rock Mechanics*. Montreal: AA Balkema, Accord, MA, US; 1987:337–342.

[39] Chen G, Zheng L, Zhang Y, Wu J. Numerical simulation in rockfall analysis: a close comparison of 2-D and 3-D DDA. *Rock Mech Rock Eng*. 2013;46:527–541. doi:10.1007/s00603-012-0360-9.

[40] Brandenberg SJ, Zhang J, Kashigahndi P, Huo Y, Zhao M. *Demand Fragility Surfaces for Bridges in Liquefied and Laterally Spreading Ground*. Berkeley, CA, US: Pacific Earthquake Engineering Research Center, University of California. PEER Report 2011/01; 2011;1:162.

[41] Gardoni P, Der Kiureghian A, Mosalam KM. *Probabilistic Models and Fragility Estimates for Bridges Components and Systems*. Berkeley, CA, US: Pacific Earthquake Engineering Research Center (PEER), University of California. Report 2002/13; 2002;1:164.

[42] Brando G, De Matteis G, Spacone E. Predictive model for the seismic vulnerability assessment of small historic centres: application to the inner Abruzzi region in Italy. *Eng Struct*. 2017;153:81–96. doi:10.1016/j.engstruct.2017.10.013.

[43] De Matteis G, Brando G, Corlito V. Predictive model for seismic vulnerability assessment of churches based on the 2009 L'Aquila earthquake. *Bull Earthquake Eng*. 2019;17:4909–4936. doi:10.1007/s10518-019-00656-7.

[44] Xie R, Fan W, Liu B, Shen D. Dynamic behavior and vulnerability analysis of bridge columns with different cross-sectional shapes under rockfall impacts. *Structures*. 2020;26:471–486. doi:10.1016/j.istruc.2020.04.042.

[45] Blitzstein JK, Hwang J. *Introduction to Probability. Texts in Statistical Science Series*. London, UK: Chapman & Hall/CRC Press, Taylor and Francis Group; 2015:570.

[46] Locati M, Camassi R, Rovida A, et al. *Database Macrosismico Italiano (DBMI15), versione 4.0 [Data set]*. Istituto Nazionale di Geofisica e Vulcanologia (INGV). doi:10.13127/dbmi/dbmi15.4.

[47] Galadini F, Galli P. The Holocene paleoearthquakes on the 1915 Avezzano earthquake faults (central Italy): implications for active tectonics in the central Apennines. *Tectonophysics*. 1999;308:143–170.

[48] Di Naccio D, Famiani D, Liberi F, et al. Site effects and widespread susceptibility to permanent coseismic deformation in the Avezzano town (Fucino basin, Central Italy): constraints from detailed geological study. *Eng Geol*. 2020;270:105583. doi:10.1016/j.enggeo.2020.105583.

[49] Hashash YMA, Musgrove MI, Harmon JA, et al. DEEPSOIL 7.0, User Manual. Urbana, IL, Board of Trustees of University of Illinois at Urbana-Champaign; 2020. https://deepsoil.cee.illinois.edu/Files/DEEPSOIL_User_Manual_v7.pdf.
[50] Stucchi M, Meletti C, Montaldo V, Crowley H, Calvi GM, Boschi E. Seismic Hazard Assessment (2003–2009) for the Italian building code. *Bull Seismol Soc Am*. 2011;101(4):1885–1911. doi:10.1785/0120100130.
[51] D'Elia B. Technical Report–Texas Instruments Italia, stabilimento di Avezzano (AQ); 1989.